



# Investigation of the marginal fit of a 3D-printed three-unit resin prosthesis with different build orientations and layer thicknesses

Min-Seong Yang, Seong-Kyun Kim\*, Seong-Joo Heo, Jai-Young Koak, Ji-Man Park

Department of Prosthodontics & Dental Research Institute, Seoul National University Dental Hospital, School of Dentistry, Seoul National University, Seoul, Republic of Korea

## ORCID

Min-Seong Yang

<https://orcid.org/0000-0002-0893-1999>

Seong-Kyun Kim

<https://orcid.org/0000-0001-8694-8385>

Seong-Joo Heo

<https://orcid.org/0000-0003-0699-4141>

Jai-Young Koak

<https://orcid.org/0000-0002-0190-0778>

Ji-Man Park

<https://orcid.org/0000-0003-0018-1166>

## Corresponding author

Seong-Kyun Kim

Department of Prosthodontics & Dental Research Institute, Seoul National University Dental Hospital, School of Dentistry, Seoul National University, 28 Yeongun-dong, Chongno-gu, Seoul, 03080, Republic of Korea

Tel +82220723860

E-mail [ksy0617@snu.ac.kr](mailto:ksy0617@snu.ac.kr)

Received April 21, 2022 /

Last Revision August 17, 2022 /

Accepted August 22, 2022

This research was supported by Basic Science Research Program through the National Research Foundation of Korea (NRF) funded by the Ministry of Education (NRF-2018R1D1A1B07042333) and by the Korea Medical Device Development Fund grant funded by the Korea government (the Ministry of Science and ICT, the Ministry of Trade, Industry and Energy, the Ministry of Health & Welfare, Republic of Korea, the Ministry of Food and Drug Safety) (Project Number: 202011A02). The authors declared no conflicts of interests.

**PURPOSE.** The purpose of this study was to analyze the marginal fit of three-unit resin prostheses printed with the stereolithography (SLA) method in two build orientations (45°, 60°) and two layer thicknesses (50 µm, 100 µm). **MATERIALS AND METHODS.** A master model for a three-unit resin prosthesis was designed with two implant abutments. Forty specimens were printed using an SLA 3D printer. The specimens were printed with two build orientations (45°, 60°), and each orientation was printed with two layer thicknesses (50 µm, 100 µm). The marginal fit was measured as the marginal gap (MG) and absolute marginal discrepancy (AMD), and MG and AMD measurements were performed at 8 points per abutment, for 16 points per specimen. All statistical analyses were performed using SPSS software. Two-way analysis of variance (ANOVA) was separately performed on the MG and AMD values of the build orientations and layer thicknesses. Moreover, one-way ANOVA was performed for each point within each group. **RESULTS.** The margins of the area adjacent to the pontic showed significantly high values, and the values were smaller when the build orientation was 45° than when it was 60°. However, the margin did not differ significantly according to the layer thicknesses. **CONCLUSION.** The marginal fit of the three-unit resin prosthesis fabricated by the SLA 3D method was affected by the pontic. Moreover, the marginal fit was affected by the build orientation. The 45° build orientation is recommended. [J Adv Prosthodont 2022;14:250-61]

## KEYWORDS

3D printing; Stereolithography; Marginal fit; Build orientation; Layer thickness

## INTRODUCTION

Digital impressions and computer-aided design (CAD)-computer-aided manufacturing (CAM) techniques have replaced traditional manufacturing meth-

© 2022 The Korean Academy of Prosthodontics

© This is an Open Access article distributed under the terms of the Creative Commons Attribution Non-Commercial License (<http://creativecommons.org/licenses/by-nc/4.0>) which permits unrestricted non-commercial use, distribution, and reproduction in any medium, provided the original work is properly cited.

ods for dental prostheses and enabled a new era of prosthesis fabrication.<sup>1</sup> The traditional fabrication method, the lost wax technique, produces a prosthesis by shaping it in wax and casting it after investing. However, that method is time-consuming and costly, and the technician's skill affects the quality of the prosthesis.<sup>2</sup> Compared with the traditional method, the CAD-CAM technique has a low learning curve and can quickly and easily fabricate prostheses of a consistent high quality, so it has been widely applied in various areas of dentistry.<sup>3</sup>

The CAM technique can use subtractive or additive manufacturing.<sup>4</sup> Subtractive manufacturing (SM) uses a milling tool to sculpt a block into the desired shape. It has disadvantages such as the waste of raw materials, wear of milling burs, and the occurrence of micro-cracks in the restorations during milling.<sup>5</sup> The additive manufacturing (AM) method, on the other hand, builds up materials into the desired shape layer by layer. As its techniques have developed, it has overcome many shortcomings of the SM method.<sup>6,7</sup> Several AM methods are used, but stereolithography (SLA) and digital light processing (DLP) are the most common. SLA polymerizes a photosensitive resin using a single focused laser.<sup>8</sup> Although the initial cost of an SLA 3D printer is high, and the printing time is longer than with a DLP 3D printer, it is widely used in dentistry because the resulting printed prostheses have high dimensional accuracy.<sup>9</sup>

Various printing parameters affect the accuracy of prostheses manufactured using CAD-CAM: build orientation, layer thickness, x-y resolution, light exposure time, post-processing, printing materials, and other factors.<sup>6</sup> Among them, many studies have examined build orientation and layer thickness. Byun and Lee<sup>10</sup> used a genetic algorithm to find the optimal orientation and improve the prototype surface roughness and build time. Zwier and Wits<sup>11</sup> found that the print orientation was a decisive factor in the quality of the printed product. To find the optimal print orientation, they minimized the overhanging and support structures using ray-tracing and convex hull methods. Singhal *et al.*<sup>12</sup> used an adaptive slicing algorithm with different slice thicknesses to improve their SLS prototype's surface roughness and geometric accuracy.

Many other studies have also been conducted to

optimize the build orientation and layer thickness, including studies on the effects of those two parameters on prosthesis fit. Park *et al.*<sup>13</sup> assessed three-unit provisional resin prostheses printed with a DLP 3D printer in ten groups (n = 10 per group) with five build orientations (0°, 30°, 45°, 60°, 90°) and two layer thicknesses (50 µm, 100 µm). Absolute marginal discrepancy (AMD), marginal gap (MG), and internal gap volume (IGV) showed the best results at build orientations of 45° and 60°, but the layer thicknesses produced different AMD, MG, and IGV results. Jang and Kim<sup>14</sup> printed three-unit resin prostheses on an SLA 3D printer and set ten groups (n = 10 for each group) using the same build orientations and layer thicknesses as in the above study to measure marginal fit and internal fit. They found that the build orientations of 45° and 60° and the 50-µm layer thickness showed the most desirable fit. Both those studies found that the build orientation and layer thickness affected the quality of the printed prostheses. However, it is necessary to check whether printed prostheses show clinically appropriate marginal fit under the conditions deemed optimal in those studies. Moreover, in those studies, margin values were measured at the 4 margin areas, but it is essential to measure margin values in more diverse areas to evaluate whether printed prostheses show clinically appropriate margin values.

Provisional restoration is an essential part of the transition period until a final restoration is delivered. It plays a role in pulp and abutment protection, positional stability, soft tissue management, and the maintenance of function and aesthetics.<sup>15</sup> Polymethyl-methacrylate (PMMA) is often used to fabricate provisional restorations. Fabricating directly in the oral cavity has various drawbacks,<sup>16</sup> particularly polymerization shrinkage and exothermic reaction. Polymerization shrinkage can cause dimensional discrepancy of the provisional prosthesis, and the exothermic reaction can inflict thermal trauma on the tooth pulp.<sup>17</sup> The indirect method for building a provisional prosthesis makes a cast from an impression of the patient's teeth, but it has the disadvantages of being affected by the technician's skill and not being reproducible.<sup>18</sup>

The most critical factor and prerequisite for ensuring the long-term success of a fixed prosthesis is mar-

ginal fit.<sup>19</sup> Adequate marginal fit has been studied by many scholars<sup>20,21</sup> because an improper marginal fit causes cement dissolution that leads to percolation of bacteria, secondary dental caries, and pulp necrosis.<sup>22</sup> Moreover, it affects the supporting periodontal tissue by causing plaque accumulation and bacterial proliferation.<sup>23</sup>

It is difficult to accurately determine a clinically acceptable margin for fixed prostheses. According to ADA standard No.8,<sup>24</sup> when using type I luting cement, the margin should not exceed 25  $\mu\text{m}$ , and when using type II luting cement, it should not exceed 40  $\mu\text{m}$ . However, satisfying those criteria in clinical situations is difficult. After examining the marginal fit of 1,000 fixed prostheses for five years, McLean and von Fraunhofer<sup>25</sup> reported that if the cement film thickness and marginal gap were less than 120  $\mu\text{m}$ , it was considered a successful prosthesis. Many clinicians agreed with that result, and many studies have used it as a clinical criterion for a successful marginal gap.<sup>18,20,26</sup>

In many cases, the same terms for marginal gap measurement have been interpreted differently. However, in 1989, Holmes *et al.*<sup>27</sup> re-established various casting misfit terms used to measure the marginal fit of prostheses, and among them, MG and AMD were widely used. Therefore, in this study, the marginal fit was measured and evaluated using MG and AMD.

The purpose of this study was to analyze the marginal fit of three-unit resin prostheses printed with the SLA method in two build orientations ( $45^\circ$ ,  $60^\circ$ ) and two layer thicknesses (50  $\mu\text{m}$ , 100  $\mu\text{m}$ ). The null hypothesis was that the marginal gap and absolute marginal discrepancy of the three-unit resin prostheses manufactured by the SLA method would not be different under the tested printing conditions.

## MATERIALS AND METHODS

A master model for a three-unit resin prosthesis with two implant abutments was designed (Fig. 1). The abutments were assumed to be mandibular second premolar and second molar, and the first molar was assumed to be the missing tooth. Each abutment was designed considering the anatomical shape and size of the teeth.<sup>28</sup> Goodacre *et al.*<sup>29</sup> argued that it was appropriate to set a total occlusal convergence angle between  $10^\circ$  and  $20^\circ$  when an occluso-cervical dimension of 4 mm was set during tooth preparation. Thus, the total convergence angle was set to  $14.3^\circ$ . The abutments were set with a 1 mm shoulder margin, and the reference points of the cone shape were designed with a diameter of 1 mm and a height of 1 mm below the margin. Reference points were set in three directions at  $90^\circ$  each and were considered to confirm the exact positional relationship during coronal and sagittal sectioning.

The standard tessellation language (STL) file of the master model was acquired using CAD software (Rhino 5.0; Robert McNeel & Associates, Seattle, WA, USA). Using the acquired STL file, a PMMA resin block (Yamahachi Dental MFG, Ochigara, Japan) was milled using a 5-axis milling machine (IDC MILL 5X; Amann Girrbach AG, Koblach, Austria). According to ISO/ASTM 52916, STL is an abbreviation of 'Stereolithography', but for connectivity with the previous studies,<sup>13,14</sup> 'Standard tessellation language' was defined as STL and 'Stereolithography' as SLA in this study.

The master model was scanned with a model scanner (T500; Medit, Seoul, Korea). According to the manufacturer, the scanning accuracy was within 7  $\mu\text{m}$ . Before scanning, anti-reflective spray (IP scan spray;

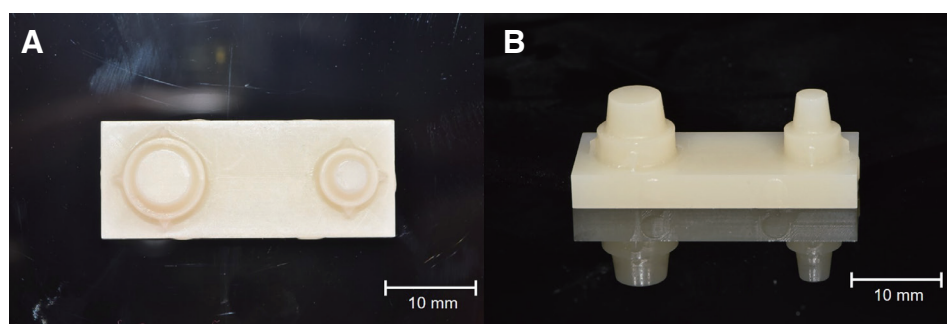


Fig. 1. The master model. (A) Occlusal view and (B) Buccal view.

IP-division, Haimhausen, Germany) was used. The scanned model was exported as an STL file. Then, the three-unit resin prosthesis was designed using the STL file and CAD software (Exocad; Darmstadt, Germany). Based on a previous study<sup>30</sup> to find an appropriate cement space for a three-unit resin prosthesis made with an SLA 3D printer, the cement space was set to 100 µm. The shape and size of the prosthesis were designed to fit the anatomical tooth morphology.<sup>28</sup>

Forty specimens were printed using an SLA 3D printer (Zenith U; Dentis, Daegu, Korea). The specifications of the SLA 3D printer are shown in Table 1. Temporary resin (ZMD-1000B temporary; Dentis, Daegu, Korea) for 3D printing was used to fabricate the specimens. The specimens were printed with two build orientations (45°, 60°) (Fig. 2), and each build orientation was used with two layer thicknesses (50 µm, 100 µm). When the build orientation was 45°, the specimens with a layer thickness of 50 µm were called Group 1, and those with a layer thickness of 100 µm were called Group 2. When the build orientation was 60°, the specimens with a layer thickness of 50 µm were called Group 3, and those with a layer thickness

**Table 1.** The specifications of the SLA 3D printer used in these experiments

Scanning method	Galvanometer
Light source	Blue laser (405 nm)
Layer thickness	16 µm, 50 µm, 100 µm
Dimension / Weight	354 × 366 × 483 mm / 17.5 kg
Working area	110 × 110 × 150 (X, Y, Z / mm)
Electrical consumption	120W
Country	Daegu, Korea
Company	Dentis

of 100 µm were called Group 4 (n = 10 per group). The details of the groups are summarized in Table 2.

According to the studies of Unkovskiy *et al.*<sup>31</sup> and Osman *et al.*,<sup>32</sup> the exposure time required for the laser to reach the specimens can be affected by their platform position, causing volume discrepancy. Therefore, four specimens were printed simultaneously to keep them the same distance from the center of the platform and facilitate printing. Supporting structures were applied automatically using Zenith

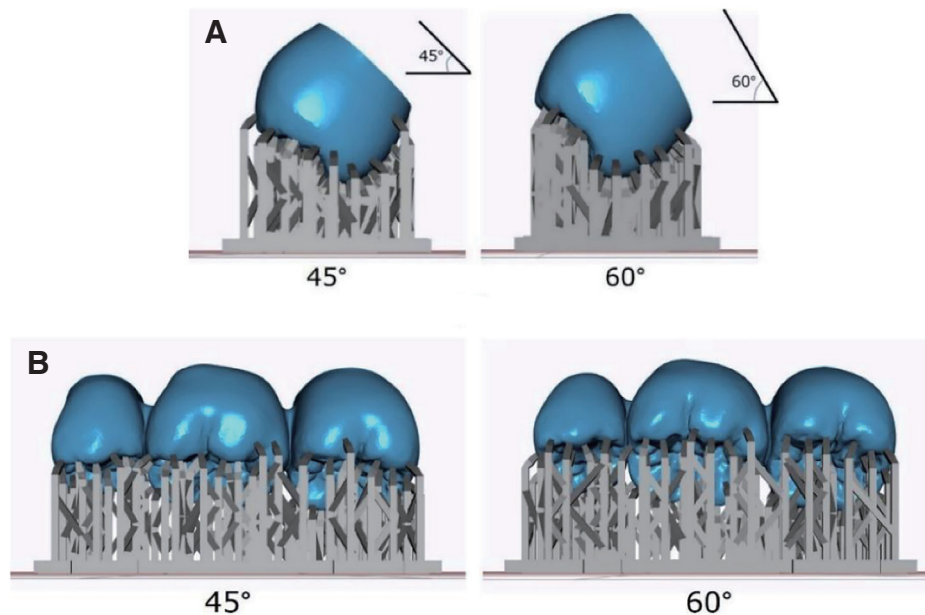


**Fig. 2.** Prosthesis design with two build orientations (45° and 60°). The connection elements of the supporting structures varied by build orientation. For example, when the build orientation was 0°, the supporting structures were vertically attached to the occlusal surface of the prosthesis, and when the build orientation was 90°, the supporting structures were vertically attached to the lingual surface of the prosthesis. (A) Distal view and (B) Buccal view.

**Table 2.** The main features of the groups designed for this experiment

	Manufacturing method	Manufacturer	Material	Build orientation	Layer thickness
Group 1	SLA method	Dentis	ZMD-1000B temporary	45°	50 $\mu\text{m}$
Group 2	SLA method	Dentis	ZMD-1000B temporary	45°	100 $\mu\text{m}$
Group 3	SLA method	Dentis	ZMD-1000B temporary	60°	50 $\mu\text{m}$
Group 4	SLA method	Dentis	ZMD-1000B temporary	60°	100 $\mu\text{m}$

printer software (Zenith S/W; Dentis, Daegu, Korea). After printing, the remaining resin was removed, and the prostheses were cleaned with 99.8% ethanol (Absolute ethanol; Koryo Chemical Eng., Seoul, Korea) for 5 minutes. Next, post-curing was performed in an ultraviolet curing unit (LC-3D Print Box; Nextdent, Utrecht, Netherlands) for 5 minutes according to the manufacturer's instruction. Then, the supporting structures were carefully removed using denture burs.

After it was confirmed that each specimen was seated on the master model without interference, the model was fixed on the jig for micro-CT scanning using a laboratory wrapping film (Parafilm; Bemis, Neenah, WI, USA) without cementation. Then, CT scanning was performed using a micro-CT scanner (Skyscan 1172; Bruker Micro CT, Billerica, MA, USA). Scanning was done using parameters based on previous studies<sup>13,14</sup>: 60 kVp and 167  $\mu\text{m}$ , with an exposure time of 1475 ms. An aluminum filter (5 mm) was used, and the resolution of the CT scan was 15.43  $\mu\text{m}$ . Each specimen was rotated 180° with 0.7° rotational steps and 3-frame averaging.

The CT data were reconstructed using NRecon soft-

ware (NRecon 1.7.4.2 version; Bruker Micro CT, Billerica, MA, USA). The threshold for the defect pixel mask was set to 3%. Ring artifact reduction was set to 8, and smoothing was set to 3. ImageJ software (ImageJ 1.52 version; NIH, Bethesda, MD, USA) was used to measure the marginal fit as the marginal gap (MG) and absolute marginal discrepancy (AMD). According to Holmes *et al.*,<sup>27</sup> MG is "the perpendicular measurement from the margin of the casting to the axial wall of the preparation," and AMD is "the angular combination of the vertical marginal discrepancy and the horizontal marginal discrepancy" (Fig. 3). Three reference points per abutment in the master model (A to F) were used for sectioning (Fig. 4). To find the desired plane, the coronal and sagittal planes were sectioned with DataViewer software (DataViewer 1.5.6.2 version; Bruker Micro CT, Billerica, MA, USA) based on the reconstructed data.

MG and AMD measurements were taken at 8 points per abutment (16 points per specimen). In the premolar, the margin on the buccal side, which was the closest to reference point C, was set as P1, and as the specimen was rotated clockwise by 45°, the margin was set as P2, P3, ..., P8. In the molar, the margin on

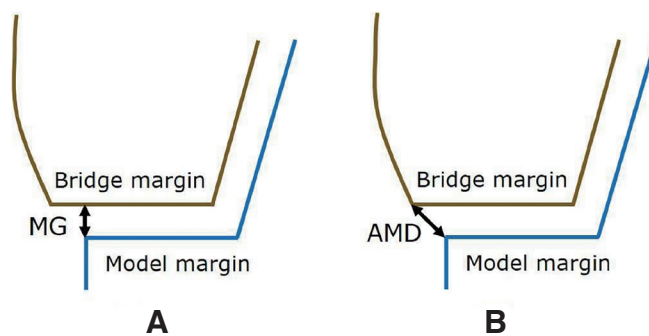


**Fig. 3.** (A) Marginal gap (MG) and (B) Absolute marginal discrepancy (AMD). The marginal fit at each margin point of the prostheses was measured using both MG and AMD.





**Fig. 4.** Reference points from A to F. For accurate margin measurement, the reference points were used for sectioning the reconstructed CT data in the desired planes.



**Fig. 5.** Margin points for each abutment. Sixteen margins per specimen were measured. Based on the center of the abutment, the margin was set to be 45° different from the adjacent margin. Margin points in the premolar were set in clockwise order, and margin points in the molar were set in counter-clockwise order.

the buccal side, which was the closest to reference point D, was set as M1, and when the specimen was rotated counter-clockwise by 45°, the margin was set as M2, M3, ..., M8 (Fig. 5).

To make the MG and AMD measurements at 16 points, seven sections per specimen had to be made. The plane passing through reference points A and B perpendicular to the master model was defined as the coronal section. The plane passing through reference points C and E perpendicular to the master model was defined as the premolar sagittal section. The plane passing through reference points D and F perpendicular to the master model was defined as the molar sagittal section. The remaining four sections were obtained by rotating the specimen 45° counter-clockwise. In the premolar, the plane connecting the longest axis to the coronal was defined as the premolar 45° coronal section. The plane connecting the longest axis to the sagittal was defined as the premolar 45° sagittal section. Likewise, in the molar, the plane con-

**Table 3.** Margin points measured in each section

Section	Premolar	Molar
Coronal section	P3, P7	M3, M7
Premolar sagittal section	P1, P5	
Molar sagittal section		M1, M5
Premolar 45° coronal section	P4, P8	
Premolar 45° sagittal section	P2, P6	
Molar 45° coronal section		M2, M6
Molar 45° sagittal section		M4, M8

necting the longest axis to the coronal was defined as the molar 45° coronal section, and the plane connecting the longest axis to the sagittal was defined as the molar 45° sagittal section. The margin points measured in each section are summarized in Table 3.

All measurements were taken under magnification of x100. Each measurement was repeated three times, and the average value was used.

For the printed prostheses, the MG and AMD values were each measured for 16 margin points. Each group was tested for normality using the Shapiro-Wilk test and for homogeneity of variance using Levene's test. All statistical analyses were performed using SPSS software (SPSS version 25; IBM, Armonk, NY, USA).

Two-way analysis of variance (ANOVA) was separately performed on the MG and AMD values for the build orientations and layer thicknesses to check the interaction effect and significance of each factor. Moreover, one-way ANOVA was performed for the MG and AMD values at each point within each group. Post hoc testing was performed using the Tukey test. The confidence level was set at 95% ( $\alpha = 0.05$ ).

## RESULTS

The MG values are shown in Figure 6. In the premolar, the smallest value was  $51.8 \pm 10.6 \mu\text{m}$  at P6 (Group 1), and the largest value was  $126.3 \pm 16.1 \mu\text{m}$  at P4 (Group 3). The points at which the value exceeded  $120 \mu\text{m}$  were P4 in Group 3 and P4 in Group 4. In the molar, the smallest value was  $48.9 \pm 6.3 \mu\text{m}$  at M7 (Group 1), and the largest value was  $127.4 \pm 12.6 \mu\text{m}$  at M4 (Group 3). The only value that exceeded  $120 \mu\text{m}$  was M4 in Group 3. The AMD values are also shown in

Figure 6. In the premolar, the smallest value was  $54.6 \pm 9.7 \mu\text{m}$  at P6 (Group 1), and the largest value was  $127.3 \pm 16.0 \mu\text{m}$  at P4 (Group 3). The points at which the value exceeded  $120 \mu\text{m}$  were P4 in Group 3 and P4 in Group 4, which is the same pattern seen with the MG. In the molar, the smallest value was  $60.1 \pm 6.8 \mu\text{m}$  at M7 (Group 4), and the largest value was  $128.5 \pm 14.2 \mu\text{m}$  at M2 (Group 3). Points at which the value exceeded  $120 \mu\text{m}$  were present in all groups: M3 and M4 in Group 1; M4 in Group 2; M2, M3, and M4 in Group 3; and M3 in Group 4. Furthermore, The MG and AMD values were analyzed for each point within each group. Regardless of the group and margin (MG or AMD), the results were somewhat consistent. Overall, P2, P3, and P4 in the premolar had significantly larger

values than the other points, and M2, M3, and M4 in the molar had significantly larger values than the other points (Fig. 6). Although it did not always show a statistically significant difference, P4 tended to show larger values than P2 and P3, and M4 tended to show larger values than M2 and M3.

The MG values differed significantly according to the build orientation. Smaller MG values were shown when the build orientation was  $45^\circ$  than when it was  $60^\circ$  ( $P = .002$ ). However, the MG values did not differ significantly according to the layer thickness ( $P = .681$ ), though there was an interaction effect between the build orientations and layer thicknesses ( $P < .001$ ) (Fig. 7A). The AMD values showed the same pattern as the MG values. Smaller AMD values were found when

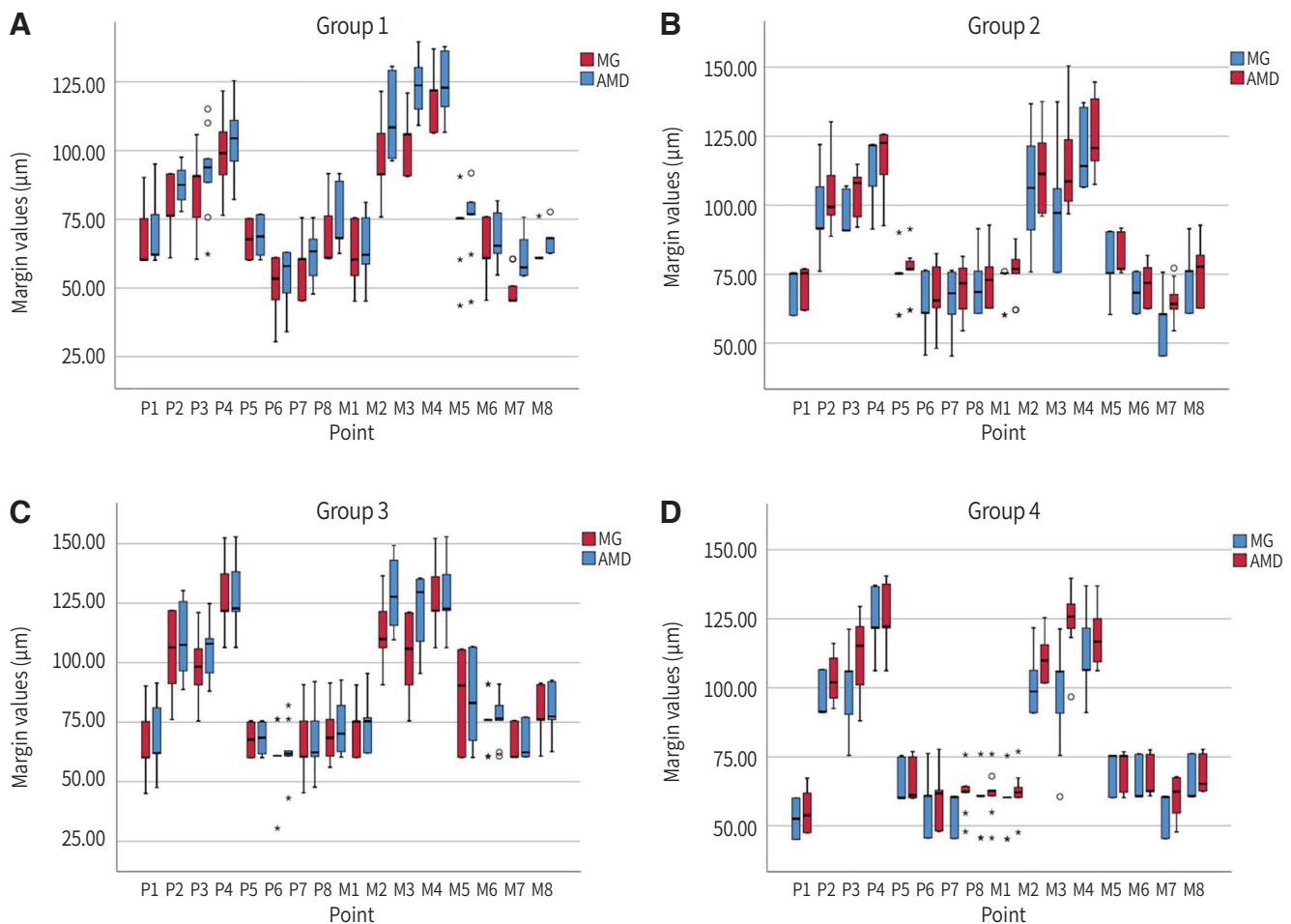


**Fig. 6.** Comparison of MG and AMD values by point within the groups. (A) Group 1 (build orientation:  $45^\circ$ , layer thickness:  $50 \mu\text{m}$ ), (B) Group 2 (build orientation:  $45^\circ$ , layer thickness:  $100 \mu\text{m}$ ), (C) Group 3 (build orientation:  $60^\circ$ , layer thickness:  $50 \mu\text{m}$ ), (D) Group 4 (build orientation:  $60^\circ$ , layer thickness:  $100 \mu\text{m}$ ). Although there were some exceptions, P2, P3, and P4 showed significantly larger values than the other points in the premolar, and M2, M3, and M4 showed significantly larger values than the other points in the molar. MG and AMD denote Marginal gap and Absolute marginal discrepancy, respectively.

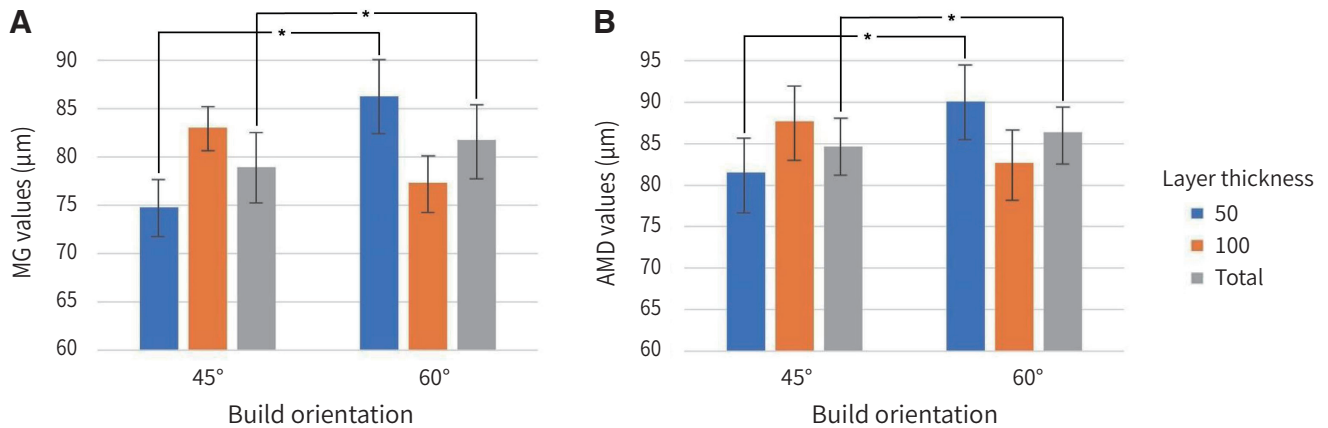


**Fig. 7.** Comparison of the effects of the build orientations and layer thicknesses. (A) MG values and (B) AMD values. Both the MG and AMD values showed significant differences according to the build orientation, with the 45° build orientation showing significantly smaller values than 60°. However, there were no differences according to the layer thickness. *P* values are listed on the graph for *P* < .05 (\*). The error bars represent the standard deviations (SD). MG and AMD denote Marginal gap and Absolute marginal discrepancy, respectively.

the build orientation was 45° than when it was 60° (*P* = .042), the AMD values did not differ significantly according to the layer thicknesses (*P* = .479), and there was an interaction effect between the build orientations and layer thicknesses (*P* < .001) (Fig. 7B).

## DISCUSSION

This study analyzed the marginal fit of three-unit resin prostheses fabricated with an SLA 3D printer using two build orientations and two layer thicknesses. The marginal fit was measured separately at 8 points in the premolar and molar, for a total of 16 points. Based on McLean's study,<sup>25</sup> 120 µm was set as a clinically acceptable margin for prostheses, and based on Holmes *et al.*'s study,<sup>27</sup> marginal fit was evaluated using the MG and AMD. The null hypothesis was rejected because points in the margins of the three-unit resin prostheses showed differences in both MG values and AMD values.

No previous study analyzed the various margin points of 3D-printed three-unit resin prostheses from both the MG and AMD aspects. In this study, the MG values ranged from 51.8 µm to 126.3 µm in the premolar and 48.9 µm to 127.4 µm in the molar, and the AMD values ranged from 54.6 µm to 127.3 µm in the premolar and 60.1 µm to 128.5 µm in the molar.

Points exceeding 120 µm were observed in both the premolar and molar, and the frequency was higher in the molar than the premolar. In the premolar, it exceeded 120 µm only at P4, but in the molar, it exceeded 120 µm at M2, M3, and M4.

Although there were some exceptions, P2, P3, P4 in the premolar and M2, M3, M4 in the molar showed significantly larger margin values than the other points. It should be noted that these points were adjacent to the pontic. Furthermore, P4 and M4 tended to show larger values than P2 and P3 and M2 and M3, respectively, although those differences were not statistically significant.

The significantly large values found in the margins adjacent to the pontic seem to be due to polymerization shrinkage of the resins used in this experiment. The amount of resin used for the pontic was larger than the amount used for each abutment, and as the amount of resin increases, the polymerization shrinkage also increases.<sup>33</sup> Moreover, referring to previous experimental results showing that the polymerization shrinkage of the resin occurred in the inward direction,<sup>34</sup> it could be expected that polymerization shrinkage in the pontic might have affected the marginal fit of the prosthesis in the area adjacent to it.

Polymerization shrinkage occurs in resins used to fabricate provisional crowns, and casting shrinkage



occurs in the metal alloys often used as the final restoration materials. The casting shrinkage of metal alloys can compensate for shrinkage caused by investment expansion, but the shrinkage of resins cannot. Although the degree of casting shrinkage varies with the metal's composition, it is about 2.1% for regular gold inlays, 2.0% for crowns, and 1.9% for MOD inlays.<sup>35</sup> In non-precious metal alloys, casting shrinkage of about 3.4% occurs because casting is performed at high temperatures.<sup>36</sup> Although polymerization shrinkage in resin depends on the main component, filler content, and polymerization method, PMMA, which is the most common material used in temporary restorations, has polymerization shrinkage of 4.5 - 6.4%.<sup>37</sup> Urethane dimethacrylate (UDMA) was the main component of the ZMD-1000B temporary resin used in this experiment, and it offers better marginal discrepancy than PMMA because it generates less heat and polymerization shrinkage.<sup>38</sup> Nonetheless, the UDMA resin still had more polymerization shrinkage than the casting shrinkage of the alloys,<sup>39</sup> which might have caused relatively more marginal discrepancy. Thus, the effect of the polymerization shrinkage of the resin on marginal discrepancy was significant. Moreover, as the amount of resin increases, the degree of polymerization shrinkage also increases,<sup>33</sup> which likely explains why the margin near the pontic in this experiment often exceeded 120  $\mu\text{m}$ .

Meanwhile, the influence of the supporting structures is apparently why P4 and M4 tended to have larger MG and AMD values than P2 and P3 and M2 and M3, respectively. The resin on the 3D-printer platform was light-cured beginning with the part closest to the platform. Because the supporting structures were directly connected to the specimen, the polymerization shrinkage in those supporting structures might have affected the specimen. However, the resin volumes in the supporting structures adjacent to the margin were a little smaller than those in the pontic, which could explain why those differences were not statistically significant. Depending on the build orientation set in this experiment (45°, 60°), many of the supporting structures were located on the lingual, occlusal surfaces. The marginal points close to the lingual surface were P4, P5, P6 in the premolar and M4, M5, M6 in the molar. Considering that those points did not differ sig-

nificantly from the other points, the polymerization shrinkage of the supporting structures probably had a minor effect compared with that of the pontic. Therefore, the polymerization shrinkage of the pontic had a major effect on the margin adjacent to it, and the shrinkage of supporting structures had a minor effect on the margin adjacent to them. In the end, the polymerization shrinkage of the pontic and supporting structures caused a synergistic effect at P4 and M4.

The effect of the supporting structures was also found in other studies. Yu *et al.*<sup>40</sup> reported that the margin quality of the area near the support attachment was poor, and rough edges tended to occur in resin prostheses printed with an SLA 3D printer. In Osman's study,<sup>32</sup> which investigated the dimensional accuracy of the build orientation of dental crowns fabricated with a DLP 3D printer, the root mean square error (RMSE) was higher in the area with the support structure. In addition, Alharbi *et al.*<sup>41</sup> investigated the effect of the build angle and support thickness on SLA 3D-printed dental restorations. The smallest RMSE was obtained with a build angle of 120° (60° in this study) and thin support, and the deviation was significant when the support was thick. Further studies are needed to examine how various support structures affect the margins of 3D-printed prostheses.

Fig. 7 shows how the build orientation and layer thickness affected the MG and AMD values. Both values showed the same results, and the layer thickness caused no significant differences. However, the build orientation did cause significant differences, with significantly smaller MG and AMD values at 45° than at 60°. In other words, the SLA 3D printer used in this experiment produced a better marginal fit when the build orientation was 45°. Similar studies of build orientation have been conducted on both DLP and SLA 3D printers. Osman *et al.*<sup>32</sup> evaluated the effect of 9 build orientations on full coverage crowns printed with a DLP 3D printer, and the dimensional accuracy was best when the build orientation was 135° (45° in this study). Unkovskiy *et al.*<sup>31</sup> evaluated bar-shaped specimens printed with an SLA 3D printer using three build orientations and reported that the printing accuracy was best at 45°. The finding of a better marginal fit at a build orientation of 45° reported here was expected for two reasons.

First, the supporting structures were positioned closer to the lingual margin when the build orientation of the prosthesis was at 60° than when it was at 45°. Therefore, polymerization shrinkage in the supporting structures was more likely to have a greater effect when the build orientation was 60°, and that was assumed to adversely affect the marginal fit.<sup>40</sup>

Second, the build orientation affected the number of slices (layers) that were polymerized,<sup>42</sup> with more layers polymerized at 60° than at 45°. Errors between layers accumulate as the number of layers increases, which could affect the accuracy of the final printed prosthesis. A result similar to this experiment was confirmed in another study<sup>14</sup> that examined the fit of three-unit resin prostheses made on an SLA 3D printer and found a significantly poorer marginal fit at 60° than at 45°.

Unlike the build orientation, the layer thickness did not cause significant differences in marginal fit. Although many studies have examined the layer thickness of 3D printers, they have often shown conflicting results. Favero *et al.*<sup>43</sup> measured the printing accuracy of an orthodontic model using three layer thicknesses (25 µm, 50 µm, and 100 µm) on an SLA 3D printer. The largest average deviation was found at 25 µm, and the smallest was found at 100 µm. However, Zhang *et al.*<sup>44</sup> reported that the average absolute deviation of orthodontic models printed with SLA and DLP 3D printers was the lowest when the layer thickness was 25 µm with SLA and 50 µm with DLP. These conflicting results indicate the need for additional, precise experiments on the effect of layer thickness.

The interaction effect between the build orientation and layer thickness was significant in both the MG and AMD values. Group 1 (build orientation: 45°, layer thickness 50 µm) and Group 4 (build orientation: 60°, layer thickness : 100 µm) had the best marginal fit, which was similar to Park's study.<sup>13</sup> This might be seen to indicate that a layer thickness offering a better marginal fit for each build orientation exists. However, because these fragmentary results alone are insufficient to derive that conclusion, studies on various combinations of build orientation and layer thickness with more diverse types of prostheses and 3D printers are needed.

Marginal fit measurements have been performed using various methods. According to a review paper<sup>45</sup>

on the margin measurement method, the most-used method is the direct view technique, followed by the cross-sectioning method, and then the replica technique. The direct view technique measures the margin using a microscope or scanning electron microscope and has the advantage of being relatively simple and not requiring additional steps.<sup>46</sup> However, it is difficult to measure a rounded margin and find an exact point.<sup>47</sup> The cross-sectioning method enables accurate margin measurement by sectioning the sample at the desired angle, but the sample must be sacrificed, and the number of sectioning planes is limited.<sup>48</sup> The replica technique obtains a fragile cement space by seating the crown using light body silicone and fixing the light body silicone using heavy body silicone. Then, the margin of the desired area is measured by sectioning. The drawback of this method is that the replica can be torn or deformed when the silicone materials are removed from the crown.<sup>49</sup> In this experiment, micro-CT was used because it can measure the margin through a three-dimensional high-resolution image without causing any damage to the specimen.<sup>26</sup> Moreover, unlike the cross-sectioning method, it is possible to use as many sections as desired from various angles to measure many margin points.<sup>16</sup>

Instead of cementing the prosthesis to the abutment, it was fixed to the micro-CT jig using wrapping film. Gonzalo *et al.*<sup>19</sup> reported a slight increase in the margin after cementation, but it was not a statistically significant difference. However, the use of cement can result in improper prosthesis seating and worsen the marginal fit.<sup>50</sup> In addition, it was reported that the radiopacity of the luting agent could interfere with the margin measurement.<sup>1</sup>

## CONCLUSION

Within the limitations of this study, the following conclusions are drawn. The marginal fit was affected by the build orientation, and a build orientation of 45° is recommended. Specifically, the marginal fit of three-unit resin prostheses fabricated by the SLA 3D-printing method was poor in the marginal areas adjacent to the pontic. The comparison of different layer thicknesses did not show a significant result, so an additional research is needed.

## REFERENCES

1. Boitelle P, Mawussi B, Tapie L, Fromentin O. A systematic review of CAD/CAM fit restoration evaluations. *J Oral Rehabil* 2014;41:853-74.
2. Abduo J, Lyons K, Bennamoun M. Trends in computer-aided manufacturing in prosthodontics: a review of the available streams. *Int J Dent* 2014;2014:783948.
3. Leeson D. The digital factory in both the modern dental lab and clinic. *Dent Mater* 2020;36:43-52.
4. Torabi K, Farjood E, Hamedani S. Rapid prototyping technologies and their applications in prosthodontics, a review of literature. *J Dent (Shiraz)* 2015;16:1-9.
5. van Noort R. The future of dental devices is digital. *Dent Mater* 2012;28:3-12.
6. Alharbi N, Wismeijer D, Osman RB. Additive manufacturing techniques in prosthodontics: where do we currently stand? a critical review. *Int J Prosthodont* 2017;30:474-84.
7. Beuer F, Schweiger J, Edelhoff D. Digital dentistry: an overview of recent developments for CAD/CAM generated restorations. *Br Dent J* 2008;204:505-11.
8. Nayar S, Bhuminathan S, Bhat WM. Rapid prototyping and stereolithography in dentistry. *J Pharm Bioallied Sci* 2015;7:S216-9.
9. Della Bona A, Cantelli V, Britto VT, Collares KF, Stansbury JW. 3D printing restorative materials using a stereolithographic technique: a systematic review. *Dent Mater* 2021;37:336-50.
10. Byun HS, Lee KH. Determination of the optimal part orientation in layered manufacturing using a genetic algorithm. *Int J Product Res* 2005;43:2709-24.
11. Zwier MP, Wits WW. Design for additive manufacturing: automated build orientation selection and optimization. *Procedia Cirp* 2016;55:128-33.
12. Singhal SK, Jain PK, Pandey PM. Adaptive slicing for SLS prototyping. *Computer-Aided Des Appl* 2008;5:412-23.
13. Park GS, Kim SK, Heo SJ, Koak JY, Seo DG. Effects of printing parameters on the fit of implant-supported 3D printing resin prosthetics. *Materials (Basel)* 2019;12:2533.
14. Jang GJ, Kim SK. Fit analysis of the stereolithography-manufacturing three-unit resin prosthesis with various 3D-printing build orientations and layer thicknesses. PhD Thesis. Seoul National University Graduate School, 2021.
15. Wu J, Xie H, Sadr A, Chung KH. Evaluation of internal fit and marginal adaptation of provisional crowns fabricated with three different techniques. *Sensors (Basel)* 2021;21:740.
16. Peng CC, Chung KH, Yau HT, Ramos V Jr. Assessment of the internal fit and marginal integrity of interim crowns made by different manufacturing methods. *J Prosthet Dent* 2020;123:514-22.
17. Mai HN, Lee KB, Lee DH. Fit of interim crowns fabricated using photopolymer-jetting 3D printing. *J Prosthet Dent* 2017;118:208-15.
18. Lee WS, Lee DH, Lee KB. Evaluation of internal fit of interim crown fabricated with CAD/CAM milling and 3D printing system. *J Adv Prosthodont* 2017;9:265-70.
19. Gonzalo E, Suárez MJ, Serrano B, Lozano JF. A comparison of the marginal vertical discrepancies of zirconium and metal ceramic posterior fixed dental prostheses before and after cementation. *J Prosthet Dent* 2009;102:378-84.
20. Yeo IS, Yang JH, Lee JB. In vitro marginal fit of three all-ceramic crown systems. *J Prosthet Dent* 2003;90:459-64.
21. Holmes JR, Sulik WD, Holland GA, Bayne SC. Marginal fit of castable ceramic crowns. *J Prosthet Dent* 1992;67:594-9.
22. Burns DR, Beck DA, Nelson SK; Committee on Research in Fixed Prosthodontics of the Academy of Fixed Prosthodontics. A review of selected dental literature on contemporary provisional fixed prosthodontic treatment: report of the Committee on Research in Fixed Prosthodontics of the Academy of Fixed Prosthodontics. *J Prosthet Dent* 2003;90:474-97.
23. Vojdani M, Torabi K, Farjood E, Khaledi A. Comparison the marginal and internal fit of metal copings cast from wax patterns fabricated by CAD/CAM and conventional wax up techniques. *J Dent (Shiraz)* 2013;14:118-29.
24. American Dental Association. ANSI/ADA Specification No. 8 for zinc phosphate cement. *Guide to dental materials and devices* 1971;1970-1.
25. McLean JW, von Fraunhofer JA. The estimation of cement film thickness by an in vivo technique. *Br Dent J* 1971;131:107-11.
26. Neves FD, Prado CJ, Prudente MS, Carneiro TA, Zancopé K, Davi LR, Mendonça G, Cooper LF, Soares CJ.

- Micro-computed tomography evaluation of marginal fit of lithium disilicate crowns fabricated by using chairside CAD/CAM systems or the heat-pressing technique. *J Prosthet Dent* 2014;112:1134-40.
27. Holmes JR, Bayne SC, Holland GA, Sulik WD. Considerations in measurement of marginal fit. *J Prosthet Dent* 1989;62:405-8.
  28. Brand RW, Isselhard DE. *Anatomy of Orofacial Structures-Enhanced 7th Edition-E-Book: A Comprehensive Approach*. Elsevier Health Sciences, 2014.
  29. Goodacre CJ, Campagni WV, Aquilino SA. Tooth preparations for complete crowns: an art form based on scientific principles. *J Prosthet Dent* 2001;85:363-76.
  30. Jang GJ, Kim SK, Heo SJ, Koak JY, Park JM. Investigation of optimal cement space in 3D printed 3-unit resin prosthesis: a pilot study. *Implantology* 2020;24:62-75.
  31. Unkovskiy A, Bui PHB, Schille C, Geis-Gerstorfer J, Huettig F, Spintzyk S. Objects build orientation, positioning, and curing influence dimensional accuracy and flexural properties of stereolithographically printed resin. *Dent Mater* 2018;34:e324-33.
  32. Osman RB, Alharbi N, Wismeijer D. Build angle: does it influence the accuracy of 3D-printed dental restorations using digital light-processing technology? *Int J Prosthodont* 2017;30:182-8.
  33. Rakhshan, V. Marginal integrity of provisional resin restoration materials: A review of the literature. *Saudi J Dent Res* 2015;6:33-40.
  34. Huang Q, Zhang J, Sabbaghi A, Dasgupta T. Optimal offline compensation of shape shrinkage for three-dimensional printing processes. *IIE trans* 2015;47:431-41.
  35. Fusayama, T. Factors and technique of precision casting part II. *J Prosthet Dent* 1959;9:486-97.
  36. Kelly JR, Rose TC. Nonprecious alloys for use in fixed prosthodontics: a literature review. *J Prosthet Dent* 1983;49:363-70.
  37. Danesh G, Lippold C, Mischke KL, Varzideh B, Reinhardt KJ, Dammaschke T, Schäfer E. Polymerization characteristics of light- and auto-curing resins for individual splints. *Dent Mater* 2006;22:426-33.
  38. Filho JD, Poskus LT, Guimarães JG, Barcellos AA, Silva EM. Degree of conversion and plasticization of dimethacrylate-based polymeric matrices: influence of light-curing mode. *J Oral Sci* 2008;50:315-21.
  39. Tjan AH, Castelnuovo J, Shiotsu G. Marginal fidelity of crowns fabricated from six proprietary provisional materials. *J Prosthet Dent* 1997;77:482-5.
  40. Yu BY, Son K, Lee KB. Evaluation of intaglio surface trueness and margin quality of interim crowns in accordance with the build angle of stereolithography apparatus 3-dimensional printing. *J Prosthet Dent* 2021;126:231-7.
  41. Alharbi N, Osman RB, Wismeijer D. Factors influencing the dimensional accuracy of 3D-printed full-coverage dental restorations using stereolithography technology. *Int J Prosthodont* 2016;29:503-10.
  42. Taufik M, Jain PK. Role of build orientation in layered manufacturing: a review. *Int J Manuf Technol Manag* 2013;27:47-73.
  43. Favero CS, English JD, Cozad BE, Wirthlin JO, Short MM, Kasper FK. Effect of print layer height and printer type on the accuracy of 3-dimensional printed orthodontic models. *Am J Orthod Dentofacial Orthop* 2017;152:557-65.
  44. Zhang ZC, Li PL, Chu FT, Shen G. Influence of the three-dimensional printing technique and printing layer thickness on model accuracy. *J Orofac Orthop* 2019;80:194-204.
  45. Nawafleh NA, Mack F, Evans J, Mackay J, Hatamleh MM. Accuracy and reliability of methods to measure marginal adaptation of crowns and FDPs: a literature review. *J Prosthodont* 2013;22:419-28.
  46. Sorensen JA. A standardized method for determination of crown margin fidelity. *J Prosthet Dent* 1990;64:18-24.
  47. May KB, Russell MM, Razzoog ME, Lang BR. Precision of fit: the Procera AllCeram crown. *J Prosthet Dent* 1998;80:394-404.
  48. Mitchell CA, Pintado MR, Douglas WH. Nondestructive, in vitro quantification of crown margins. *J Prosthet Dent* 2001;85:575-84.
  49. Wolfart S, Wegner SM, Al-Halabi A, Kern M. Clinical evaluation of marginal fit of a new experimental all-ceramic system before and after cementation. *Int J Prosthodont* 2003;16:587-92.
  50. Mously HA, Finkelman M, Zandparsa R, Hirayama H. Marginal and internal adaptation of ceramic crown restorations fabricated with CAD/CAM technology and the heat-press technique. *J Prosthet Dent* 2014;112:249-56.